arXiv:astro-ph/0510291v1 10 Oct 2005

TESTING GLOBAL ISM MODELS: A DETAILED COMPARISON OF OVI COLUMN DENSITIES WITH FUSE AND COPERNICUS DATA

Miguel A. de Avillez[1,2] and Dieter Breitschwerdt[2]

[1]Department of Mathematics, University of Évora, R. Romão Ramalho 59, 7000 Évora, Portugal
[2] Institut für Astronomie, University of Vienna,Türkenschanzstraße 17, A-1180 Vienna, Austria
E-mail: mavillez, breitschwerdt@astro.univie.ac.at
Submitted to the Astrophysical Journal (Letters), day May 2005

ABSTRACT

We study the OVI distribution in space and time in a representative section of the Galactic disk by 3D adaptive mesh refinement HD and MHD simulations of the ISM, including the disk-halo-disk circulation. The simulations describe a supernova driven ISM on large (~ 10 kpc) and small (~ 1.25 pc) scales over a sufficiently large timescale (~ 400 Myrs) in order to establish a global dynamical equilibrium. The OVI column density, N(OVI), is monitored through lines of sight measurements at different locations in the simulated disk. One has been deliberately chosen to be inside of a hot bubble, like our own Local Bubble, while the other locations are random. We obtain a correlation between N(OVI) and distance, which is independent of the observer's vantage point in the disk. In particular, the location of the observer *inside a hot bubble* does not have any influence on the correlation, because the contribution of an individual bubble (with a typical extension of 100 pc) is negligibly small. We find a remarkable agreement between the OVI column densities (as a function of distance) and the averaged OVI density ($\sim 1.8 \times 10^{-8}$ cm^{-3}) in the disk from our simulations and the values observed with COPERNICUS, and FUSE. Our results strongly support the important rôle of turbulent mixing in the distribution of OVI clumps in the ISM. Supernova induced turbulence is quite strong and unavoidable due to shearing motions in the ISM and operates on a large range of scales.

Subject headings: Hydrodynamics – Magnetohydrodynamics – Galaxy: disk – ISM: general – ISM: kinematics and dynamics – ISM: structure

1. INTRODUCTION

Historically, the discovery of a wide-spread diffuse OVI component with the COPERNICUS satellite in absorption towards background stars, which was not attributable to the circumstellar environment, led to the establishment of the hot phase of the ISM (Rogerson et al. 1973; York 1974; Jenkins & Meloy 1974). Attempts to link this to the soft X-ray background (SXRB) discovered earlier (Bowyer et al. 1968) were doomed to fail, because the excitation temperatures were too different: collisionally ionized OVI traces gas of $\sim 3 \times 10^5$ K, whereas the SXRB monitors $\sim 10^6$ K gas. In collisional ionization equilibrium (CIE) this difference is impossible to reconcile, since at SXRB temperatures the ion fraction of OVII is dominating OVI by more than two orders of magnitude. Subsequently, the idea that OVI was produced mostly in conductive interfaces between hot and cool gas (McKee & Ostriker 1977; Cowie et al. 1979) rather than in supernova remnants gained a lot of attraction. However, heat conduction in a magnetized plasma is substantially reduced to the order of a gyroradius, perpendicular to the magnetic lines of force. If the field lines are highly tangled on small scales, as it is expected in a turbulent medium, also heat transfer parallel to the field is severely reduced by effects of electron trapping in magnetic mirrors. For a detailed discussion see Malyshkin & Kulsrud (2001) and Avillez & Breitschwerdt (2004).

The OVI distribution in the Galactic disk, within the Local Bubble (LB) and near the midplane, have been discussed by, e.g., Oegerle et al. (2005) and Bowen et al. (2005), respectively. The former authors, using FUSE data, showed that the OVI column densities, N(OVI), in absorption seen along lines of sight (LOS) against 13, of the 25 white dwarfs, located within a distance up to 130 pc from the Sun, are $< 10^{13}$ cm^{-2}. No N(OVI) exceeded 1.7×10^{13} cm^{-2}. The average OVI number density in the Local ISM found by these authors is 2.4×10^{-8} cm^{-3}, a factor 1.4 larger than the overall OVI density (1.7×10^{-8} cm^{-2}) estimated by Bowen et al. (2005), who combined FUSE absorption measurements against stars located at distances > 1 kpc with data from COPERNICUS. These results indicate that the OVI has a clumpy distribution.

In this letter we show that within the framework of the SN-driven ISM model by Avillez (2000) and Avillez & Breitschwerdt (2004, 2005; henceforth AB04 and AB05, respectively), which does not include heat conduction, both the distribution of N(OVI) and its dispersion with distance, as well as the mean OVI density in the Galactic disk agree remarkably well with observations. Our simulations emphasize the importance of turbulent diffusion as an efficient process in mixing cold and hot gas, an aspect which hitherto has not been studied in sufficient detail.

2. MODEL AND SIMULATIONS

In this study we use previously published HD and MHD (with a total field of 4.5 μG, with the mean and random components of $B_u = 3.1$ and $\delta B = 3.2$ μG, respectively) adaptive mesh refinement simulations of the SN-driven ISM. The simulations use a grid centred at the solar circle with a square disk area of 1 kpc^2 and extending from $z = -10$ to 10 kpc in the direction perpendicular to the Galactic midplane. The finest resolution is 1.25 pc. The model includes a gravitational field provided by the stars in the disk, radiative cooling assuming CIE and solar abundances (e.g., Sutherland & Dopita 1993), uniform heating due to starlight varying with z and a magnetic field (setup at time zero assuming equipartition) for the case of MHD runs. SNe types Ia and II are the sources of mass, momentum and energy. SNe Ia are randomly distributed, while SNe II have

their progenitors generated in a self-consistent way according to the mass distribution in the simulated disk and are followed kinematically according to the velocity dispersion of their progenitors. In these runs we do not consider heat conduction. For details on the setup and simulations see AB04 and AB05.

3. RESULTS

Our analysis is restricted to the disk region $|z| \leq 250$ pc. We took LOS, with 1° interval, from different positions (Figure 1) located in the midplane at coordinates (x=0, y=0) pc (Pos. A), (x=1000, y=500) pc (Pos. B), (x=200, y=800) pc (Pos. C) and (x=0, y=1000) pc (Pos. D). Position C is located inside of a hot bubble similar to our LB (right panel of Figure 2). At positions A and D we took 71 LOS covering a region of 70°, while at positions B and C we took 91 and 86 LOS spanning regions of 90° and 85°, respectively. The maximum LOS lengths are 1 kpc for positions A, B and D and 0.8 kpc for position C. The step length is 10 pc. The periodicity of the boundary conditions along the $x-$ and $y-$directions assures the continuity with surrounding regions that are not calculated, thereby not affecting the column densities near the boundaries.

The left panel of Figure 2 compares COPERNICUS (black triangles: Jenkins 1978) and FUSE (stars: Oegerle et al. 2005 and green triangles: Savage & Lehner 2005) data with N(OVI) measurements along LOS taken at positions C (red) and D (blue) at time $t = 393$ Myr. The red circles correspond to N(OVI) measurements along LOS (with lengths ≤ 150 pc) that sample gas inside the bubble centred at position C (right panel of Figure 2). These measurements show that the N(OVI) variation inside the cavity is similar to that observed with FUSE in the LB. The red and blue lines represent N(OVI) along specific LOS shown in the right panel of Figure 2, while the red triangles and blue squares correspond to spatially averaged N(OVI) over the 86 and 71 LOS taken at positions C and D, respectively (see Figure 1). These measurements indicate that: (i) for an observer located at position D (outside of a bubble) there is no detection of OVI until the LOS cross a nearby bubble, (ii) for $d > 100$ pc, i.e. a distance much larger than the typical size of a bubble, the N(OVI) correlates nicely with distance, and (iii) the N(OVI) measurements are independent of the observer's location inside of a hot bubble, because of its small contribution to the total amount of OVI sampled outside of the cavity for $d \gg 100$ pc.

A considerable amount of OVI is generated in the interiors of regions created by SNe as a result of local cooling promoted by turbulent mixing (see right panel of Figure 2, as well as the blow-up of the bubble in location C, shown in the same panel). The main advantage of turbulent mixing as compared to diffusion is the increase of the interaction surfaces between the cool/warm and hot gas, thus promoting faster cooling. Hence, the rôle of heat conduction (if permitted by a magnetic field) in these cooling interfaces will be diminished by the reduction of the temperature gradients due to the turbulent mixing.

With increasing distance there are jumps (roughly every 100 pc, indicating that the mean free path between regions with high OVI density is of this order) in the column density profiles shown in the left panel of Figure 2 indicating that OVI clumps resulting from cooling interfaces are intersected by the LOS. However, on larger scales (a few hundred pc), due to a repetition in the ISM pattern distribution of the various phases, the overall OVI distribution appears smoother (see Figure 3).

In order to see that the N(OVI) correlation with distance is

not a transient phenomenon we calculated the time average OVI column density, $\langle N(OVI) \rangle_t$, over the period 301-400 Myr using 100 data cubes separated by 1 Myr, along the 71 LOS taken at positions A and B for the HD and MHD runs. Figure 3 compares the $\langle N(OVI) \rangle_t$ in the HD and MHD runs with FUSE (stars) and COPERNICUS (triangles) data. The figure shows a remarkable overlap between the observed and simulated column densities. In particular, the N(OVI) correlation with distance is reproduced in the averaging process over a period of 100 Myr of disk evolution. Thus, such a correlation is independent of time, provided that the global (not the local) SN rate is constant with time. Furthermore, it is independent of the observer's vantage point from which the LOS, sampling gas at distances > 100 pc, are taken.

Although the OVI is distributed smoothly enough for N(OVI) to correlate with distance, the dispersion $\sigma_{N(OVI)}/\langle N(OVI) \rangle$ is independent of distance (Figure 4) once $d > 100$ pc. This result is fully consistent with observations (e.g., Bowen et al. 2005).

The average of the ratio of the $\langle N(OVI) \rangle_t$, shown in Figure 3, and the distance yields an OVI number density of $1.7 - 2.1 \times 10^{-8}$ cm^{-3} for the HD and MHD cases. This value is in agreement with the time averaged value of n(OVI)$\sim 1.81 \times 10^{-8}$ cm^{-3} found in the simulated disks during the period $100 \leq t \leq 400$ Myr (Figure 5). At time 393 Myr $\langle N(OVI) \rangle = 2 \times 10^{-8}$ cm^{-3}. The oscillations in n(OVI) around the mean value seen in the figure are correlated with local variations in the SN rate. In fact, taking into account that the number of stars during the simulations at any time are determined self-consistently from the amount of cold gas present in the disk at that time, it is not difficult to conclude that spatial variations in the star formation rate occur, generating local variations in the OVI density.

4. DISCUSSION

The picture that emerges from the present simulations is that OVI absorption arises from clumps distributed in the highly turbulent interstellar medium. As shown in this letter, without taking into account heat conduction (which will be the subject of a forthcoming paper), the simulations reproduce the OVI distribution that has been measured with FUSE and COPERNICUS. The clumpy distribution is a natural consequence of turbulent diffusion, induced by shear motions, that efficiently transports and mixes cold and hot gas inside the bubbles and at small scale interfaces. Shear motions destroy large scale surfaces of adjacent cold and hot gas by generating vorticity, which stretches the fluid into thin filaments. Therefore, the patchiness of the OVI distribution is retained, but the amount of OVI per interface is substantially reduced.

Oegerle et al. have argued that heat conduction across interfaces between clouds and hot gas generates the observed OVI distribution. But, since the process is too efficient it has to be quenched significantly by invoking tangled magnetic fields on the clouds' surfaces, resulting in a patchy distribution. Although this mechanism can in principle operate, it seems to be contrived as the quenching factors have to be assumed ad hoc to fit the data. Due to the lack of predictive power of conduction, we favour turbulent mixing, which arises naturally from a SN driven ISM, as the main process for generating OVI patches in the ISM, also explaining the data without further tuning of the model. In fact, heat conduction, depending on local temperature gradients, is usually slower than turbulent mixing. Still heat conduction can be important locally, if the magnetic field

topology permits. In a SN driven ISM, on the other hand, turbulent mixing will be inescapable, independent of the field geometry, as vortex stretching implies field line stretching down to scales where tension forces become strong enough to counteract.

The correlation of N(OVI) with distance for $d > 100$ pc indicates that the processes, which give rise to the existence of hot gas in the Galactic disk are ubiquitous in all the simulated ISM in both HD and MHD runs, and ISM patterns repeat on scales of a few 100 pc. The small contribution that hot bubbles have to the OVI distribution (and N(OVI) correlation with distance) seen in LOS sampling gas *outside* the bubbles itself, indicates that the Local Bubble has a negligible contribution to the N(OVI) measured for LOS distances > 120 pc.

It has been argued recently that the abundances in the local ISM are roughly 2/3 solar (e.g., Meyer 2001) hence, -log(O/H)=-3.46 instead of -3.07 for solar abundances (Anders & Grevesse 1989). We have therefore repeated the HD run (but for a time evolution of 250 Myr due to computing time limitations) for this case with the result of slight reductions in the OVI dispersion (black triangles in Figure 4) and in N(OVI) (see Figure 3, where the red lines show time averaged, over the period 200-250 Myr, N(OVI) measured at positions A and B). These findings can be understood if one realizes that a reduced metallicity also leads to a reduced cooling of the interstellar gas, and hence to larger cooling times. Using CIE cooling curves, the transition in the temperature range where OVI is the dominant ionization stage takes longer compared to the solar abundance case. Therefore we are likely to observe a somewhat higher amount of OVI in the supernova driven ISM, compensating to some extent the lower oxygen abundance. Our calculations do not include depletion of oxygen onto dust grains.

This might reduce N(OVI) somewhat, although we do not expect depletion in this temperature range to be very high.

5. CONCLUDING REMARKS

It should be emphasized that no "tuning" of the simulations was applied. Both HD and MHD runs and the resulting data cubes were obtained *before* we had access to the FUSE data. There are no free physical parameters in the set-up (we fixed whatever we could to observed Galactic values, e.g. diffuse photon field, gravitational field etc.). All we used was a starting model that corresponded to the *currently* observed HI and HII distribution in the Galactic disk, and a SN rate fixed initially at the current rate. Then we let the system evolve for a sufficiently long time. Therefore, either the system is very *insensitive* to physical boundary conditions, or, we have captured the major features of the ISM, resulting in a global dynamical equilibrium. Although it is true that the system is self-regulating to some extent, the first possibility could not be confirmed, since volume filling factors depend sensitively on the SN rate (especially for the hot gas) and the establishment of a Galactic fountain flow. We therefore favour the second possibility, with a corollary, that conductive interfaces, which should be abundant and exhibit a significant amount of OVI, if heat conduction is a major transport process in the ISM, are unlikely to dominate the redistribution of energy. This task is more efficiently done by turbulent mixing. A detailed study of the results discussed here, as well as on the kinematics of the OVI in the ISM, will be presented in a forthcoming paper.

REFERENCES

Anders, E., & Grevesse, N. 1989, Geochim. Cosmochim. Acta, 53, 197
Avillez, M. A. 2000, MNRAS, 315, 479
Avillez, M. A., & Breitschwerdt, D. 2004, A&A, 425, 899 (AB04)
Avillez, M. A., & Breitschwerdt, D. 2005, A&A, 436, 585 (AB05)
Bowen, D. V., et al. 2005, in "Astrophysics in the Far Ultraviolet - Five years of discovery with FUSE", eds. G. Sonneborn, W. Moos, & B.-G. Andersson, ASP Conf. [astro-ph/0410008]
Bowyer, C. S., Field, G. B., & Mack, J. F. 1968, Nature, 217, 32
Cowie, L. L., et al. 1979, ApJ, 232, 467
Cox, D. P. 2004, Ap&SS, 289, 469
Jenkins, E. B., & Meloy, D. A. 1974, ApJ, 193, L121

Jenkins, E. B. 1978, ApJ, 219, 845
Malyshkin, L., Kulsrud, R., 2001, ApJ, 549, 402
McKee, C.F., Ostriker, J.P. 1977, ApJ 218, 148
Meyer, D. M. 2001, in "Gaseous Matter in Galaxies and Intergalactic Space", eds. R. Ferlet et al., Editions Frontiers, Paris, 135
Oegerle, W. R., et al. 2005, ApJ, 622, 3770
Rogerson, J. B., et al. 1973, ApJ, 181, L110
Savage, B. D., & Lehner, N. 2005, astro-ph/0509458
Sutherland, R. S., & Dopita, M. A. 1993, ApJS, 88, 253
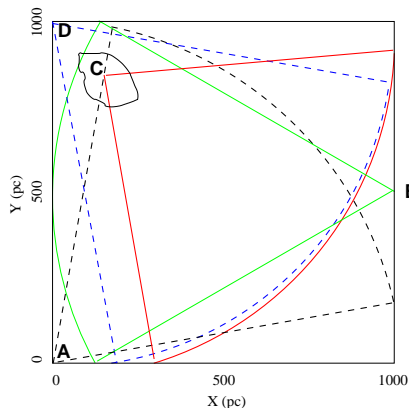York, D. G. 1974, ApJ, 193, L127

FIG. 1.— Spatial distribution, in the simulated Galactic midplane of the locations A, B, C and D, from which the lines of sight are taken and span a projected area of 90 (B), 85 (C) and 70 (A and D) degrees. The LOS cross the data cubes up to projected distances of 1 kpc for all the locations except for position C (located inside a bubble; see right panel of Figure 2), where the maximum length is only 800 pc.
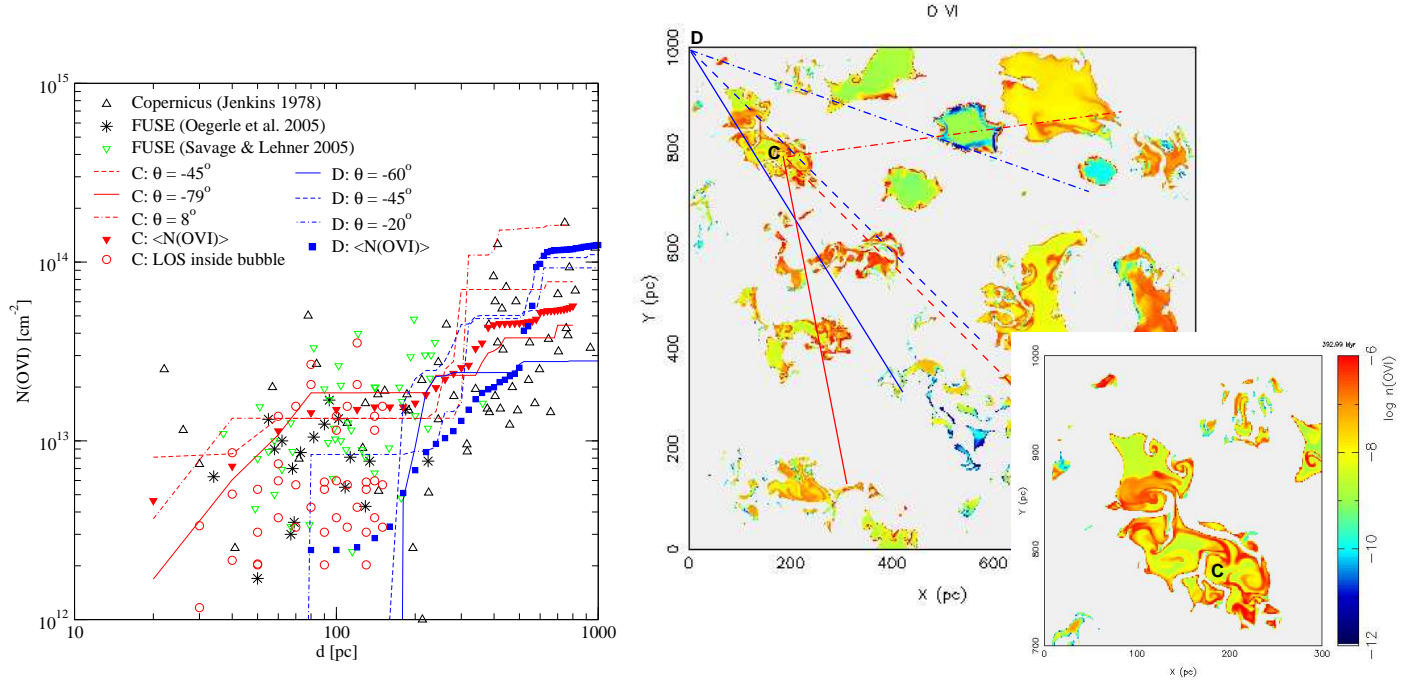
FIG. 2.— *Left panel:* Comparison of FUSE (stars: Oegerle et al. 2005; green triangles: Savage & Lehner 2005) and COPERNICUS (black triangles) OVI column densities with spatially averaged (red triangles and blue squares) and single lines of sight (red and blue lines) N(OVI) measurements in the simulated disk at time $t = 393$ Myr. The LOS are taken at positions C (red) and D (blue), which are located inside and outside of a bubble cavity, respectively, as shown in the right panel. The panel also shows N(OVI) measurements along LOS sampling gas inside the cavity (red circles) along directions other than those shown by the red lines. Note that the variation in N(OVI) inside the bubble is similar to that observed with FUSE for LOS < 150 pc. *Right panel:* OVI density distribution (in logarithmic scale) in the midplane at time $t = 393$ Myr. The panel also includes a blow-up of the bubble located in position C. The colour scale varies between 10^{-12} and 10^{-6} cm^{-3}; grey corresponds to n(OVI)$\leq 10^{-18}$ cm^{-3}. Note the eddy-like structures of OVI inside the bubbles.

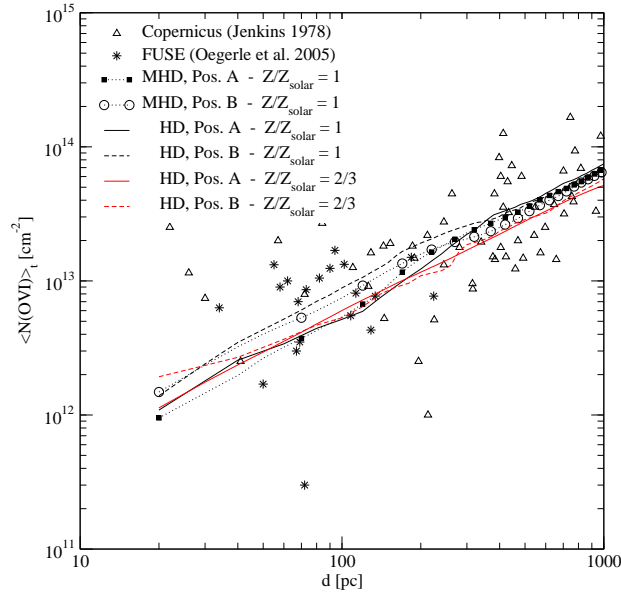
FIG. 3.— Time averaged OVI column densities, $\langle$N(OVI)$\rangle_t$, as a function of distance for HD and MHD runs with solar (black lines) and HD run with 2/3 solar (red lines) abundances, overlayed on FUSE (stars; Oegerle et al.) and COPERNICUS (triangles) data. The lines of sight were taken at positions A and B (see Figure 1). The time average is calculated over a period of 100 and 50 Myr in the cases of the solar and subsolar abundances, respectively.
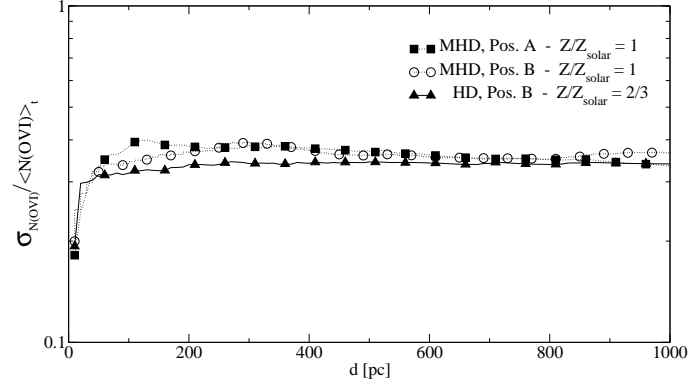
FIG. 4.— Variation with distance of the N(O VI) dispersion for the measurements at positions A and B in the MHD (solar abundances) and position B in the HD (2/3 solar abundance) runs shown in Figure 3.
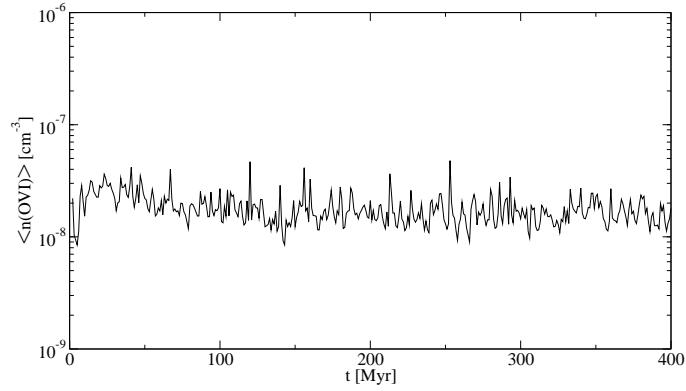

FIG. 5.— Time evolution of the $\langle$n(O VI)$\rangle$ in the simulated disk (using solar abundances). The mean of the distribution is located at $\sim 1.8 \times 10^{-8}$ cm^{-3}.